3D SEISMIC SURVEY FOR GEOTHERMAL RESERVOIR IMAGING IN THE YAMAGAWA GEOTHERMAL FIELD, SOUTHWESTERN JAPAN

Masato Fukuda[1], Naoshi Aoki[2], Kaoru Satoh[2], Takao Nibe[2], Susumu Abe[3], Toshiyuki Tosha[4]

[1]Japan Oil, Gas and Metals National Corporation, 2-10-1 Toranomon, Minato-ku, Tokyo 105-0001, Japan

[2]JGI, Inc., 1-5-21 Otsuka, Bunkyo-ku, Tokyo 112-0012, Japan

[3]Japan Petroleum Exploration Co., Ltd., 1-7-12 Marunouchi, Chiyoda-ku, Tokyo 100-0005, Japan

[4]Kumamoto University, 2-39-1 Kurokami, Chuo-ku, Kumamoto 890-8555, Japan

fukuda-masato@jogmec.go.jp

Keywords: *3D, Seismic Survey, Reflection survey, Refraction Survey, R&D, JOGMEC, Yamagawa, Japan,*

ABSTRACT

Japan Oil, Gas and Metals National Corporation (JOGMEC) is engaged in a technology development project for geothermal reservoir exploration. This project aims to develop an effective method to get an accurate image of reservoir structure, and to improve the geothermal model. Most of the geothermal reservoirs in Japan are composed of steeply dipping faults or fracture zones. Gravity and electromagnetic surveys are commonly conducted to identify reservoir structure and find caprocks and geothermal fluids. However, there is a considerable difference between these survey resolutions and distributions of faults or fracture zones detected by drilling or wellbore imaging. To fill this gap, we focused our attention on a seismic method to reveal the detailed reservoir structure with a higher spatial resolution, applying seismic method to geothermal reservoir exploration, conducting a 3D seismic reflection and refraction survey to verify the method, and obtaining experimental solutions.

The Survey was designed with goal of obtaining sufficient resolution to identify fractures and faults. We acquired data with the combination of 3,262 shot points and 4,989 receiver points and processed the data with appropriate static correction and noise reduction, which is one of the most important procedures. 3D seismic data volume was interpreted through integrating the seismic data with the well data. Estimated horizon of the upper Nansatsu formation shows consistency with the conventional geological conceptual model. We also applied coherence analysis to obtain semblance attributes that indicate the location of horizontal discontinuities of reflection events. Some indications are distributed in the injection zone and the peripheries of the intruded dacite, margins of which are detected as production zones.

1. INTRODUCTION

1.1 Background

A couple of decades ago, there were some attempts to apply seismic survey method to geothermal exploration (e.g. Horikoshi et al., 1996). However, those efforts could not accomplish expanding the use of this method in the geothermal development field. It is thought to be the cause of difficulty of acquiring high-quality data in precipitous mountain regions with a limited number of survey equipment and inadequate computational power of the time for advanced data processing. On the other hand, seismic survey technology has been astoundingly improved in oil and gas exploration field by the rapid expansion of computational power during the last decade. High performance of the computer allows to deal with an enormous quantity of seismic data and applies advanced processing algorithms with realistic man-hour. These progresses have been steadily improving images of subsurface structure.

We focused our attention on the current of seismic technology, and launched a technology development project that aimed to apply seismic method to geothermal reservoir imaging.

1.2 Geothermal Reservoir Exploration Technology Development

JOGMEC started the geothermal reservoir exploration technology development in 2013. This project aims to develop highly accurate reservoir structure imaging technology by taking 5 years. First year, we conducted survey of existing conditions to sort out problems in the application of seismic method to geothermal exploration. We also applied the modern seismic processing on a seismic data set already taken about 10 years ago and obtained an improved seismic image of steep dip fractures. (Tosha et al., 2015).

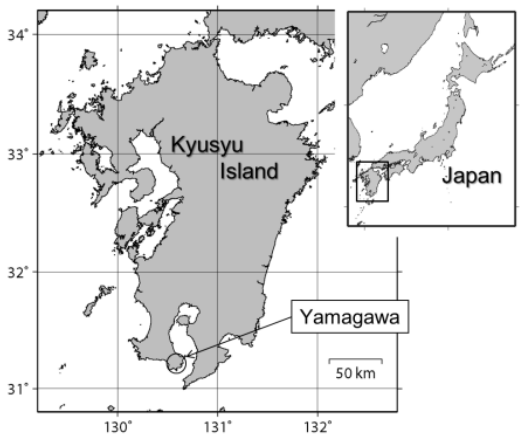

Figure 1. Location of the Yamagawa Geothermal Field.

Based on the survey results, we demonstrated the ability of the seismic survey for reservoir structure imaging. We chose Yamagawa geothermal field in Kagoshima prefecture for the verification where is the rare place located on a relatively gentle terrain among other geothermal fields (Figure 1).

Yamagawa power plant started the operation in 1995 at the center of the Yamagawa geothermal field. Kyushu Electric Power Co., Inc. operates with single flash system having 25,960 kW installed capacity. Two-phase geothermal fluid is produced by 5 active production wells (1,800 ~ 2,105m depth) and residual water is returned by 10 active reinjection wells (990 ~ 2,505m depth) (Thermal and Nuclear Power Engineering Society, 2016)

2. 3D SEISMIC SURVEY

2.1 Regional Geology and Yamagawa Geothermal Field

Yamagawa geothermal field is located on the southern part of Kyusyu Island and western side of the Ata caldera currently submerged in the Kagoshima Bay (Matumoto, 1943). There have been several small eruptions since the Tertiary until historic period. The heat source of these volcanic activities is expected to exist at the deeper part of the Ata caldera, and several magma ascents have generated lava dome along tectonic lines (e.g. Takeyama-Tsujinodake tectonic line) through the various paths.

Yoshimura et al (1985) classified the stratigraphy into six units; Kaimondake scoria, Ikeda pyroclastic flow, Takeyama andesite, Fushime silt, Yamagawa formation and Nansatsu group (from the top to the bottom). Yamagawa power station is surrounded by three faults trapezoidally and the Nansatsu group has depression structure associated with these faults (Figure 2 and 3).

Yamagawa formation covers thickly the depression structure indicated by top surface of the upper Nansatsu formation shown in purple. Dacite intrusive body is confirmed at the 2 km depths beneath the Yamagawa geothermal power plant detected by several well drillings.

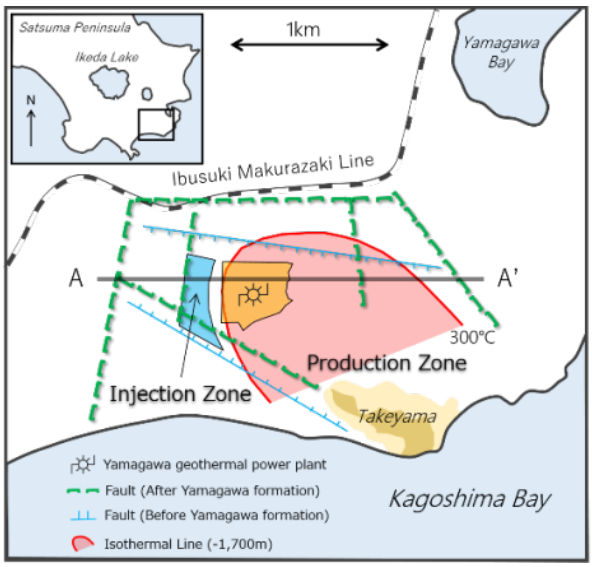

Figure 2. Composite map around Yamagawa geothermal power plant (after Sakuma, 1999) A-A' cross section is shown in Figure 3.

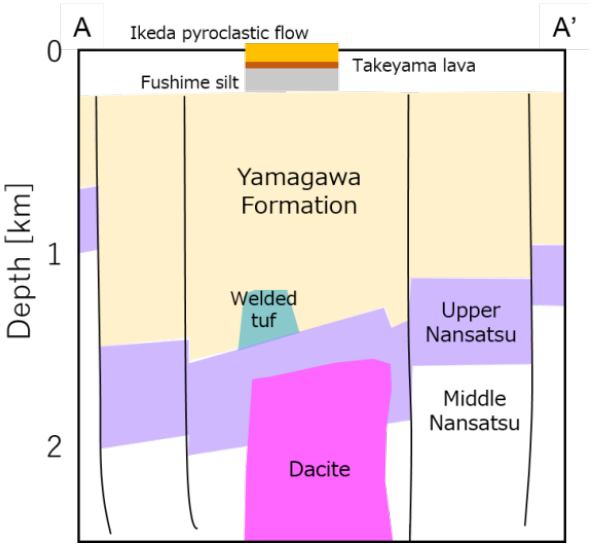

Figure 3. Geological conceptual cross section (A-A') in figure 2 (After Sakuma, 1999).

It is considered that the intrusive dacite developed the productive fracture reservoir zone while the cracking associated with intrusion and the dacite also functions as a local thermal source of the Yamagawa geothermal system. Okada et al (2000) point the high reservoir temperature over 350 degrees Celsius and a high salinity production fluid as the characteristics of Yamagawa geothermal fluids.

2.2 Survey Design

We conducted a careful survey design to achieve appropriate survey specification as was pointed out in the existing conditions survey. The survey design was optimized to image the fracture reservoir structure around the Yamagawa geothermal field. Readjusted agricultural land and road networks of Yamagawa field allowed us to expand survey lines for efficient subsurface illumination. Dense survey lines and survey points were arranged above the reservoir zone. Taper zone is added to the zone of interest for migration imaging processing. In addition to the survey lines, we distributed the marginal survey area to acquire the data for refraction velocity tomography (Figure 4).

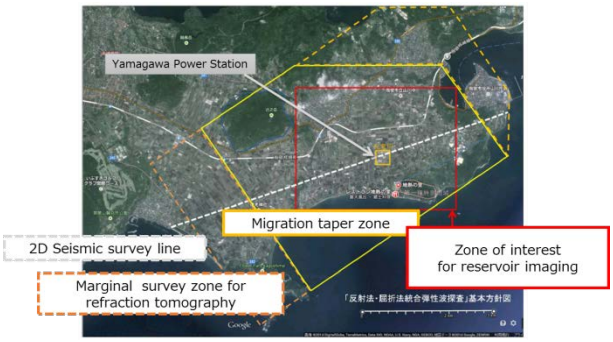

Figure 4: Basic survey policy of Yamagawa 3D seismic survey.

There are residential areas within the zone of interest, where the shooting operations and the deployment of wired geophone survey lines are limited due to a paved ground and/or a frequent traffic of local people. Data recorded in such areas

sometimes show missing gaps and reduced quality. To avoid such gap, we utilized a stand-alone geophone system to fill the restriction zones (Figure 5).

Stand-alone measurement equipment is recognized as a key technology to enhance the seismic survey in residential area and/or mountainous area, where limited roads for wired geophone lines are available (e.g., Geospace Technologies, 2012). In fact, stand-alone measurement equipments were installed in the area isolated from a survey line network due to a landslide. We have high expectation of efficacy of a stand-alone measurement system at a geothermal area that has the feature of several difficulties for seismic data acquisition.

Figure 5: Cable-less seismic recording system.

2.3 Seismic Data Acquisition

We conducted Yamagawa seismic survey from 20th August to 14th October 2015 within the scope of the optimized survey design. Survey specification is shown in Table 1.

Table 1: Survey specification of Yamagawa seismic survey

Total Survey Extension/Area	
2D Line	8km
3D Survey(Imaging)	12km²(3km × 4 km)
3D Survey(Total)	36km²(4.5km × 8km)
Receiver Specification	
Geophone Interval	
2D Line	10m
3D Survey(Imaging)	20m
3D Survey(Marginal Zone)	40m
Refraction Survey	80m
Number of Wired Geophone	
2D Line	997
3D Survey(Imaging)	1,631
3D Survey(Marginal Zone)	506
Total	3,134
Number of Cable-less Geophones	1,855
Total Number of Geophones	4,989
Recording Time	6 sec
Sampling Rate	4 ms
Shooting Specification	
Shooting Interval	
2D Line	10m
3D Survey(Imaging)	20m
3D Survey(Marginal Zone)	40m
Refraction Survey	80m
Number of Shooting	
2D Line	834
3D Survey	2,346
Refraction Survey	77
Residential Zone	5
Total	3,262
Seismic Source	Vibrator
Sweep Type	Non-Linear
Sweep Frequency	3 or 4 – 60 Hz
Sweep Length	16 sec
Number of Sweep	4-8(2D)/3-12(3D)

We took on different types of vibrator depending on the situation of shooting point. Large-size vibrator sources (18.9 ton/vehicle) were used at wide and well paved roads up to four vibrators with synchronizing their sweep signals. Middle-size vibrator sources (7.9 ton/vehicle) were used for narrow roads and/or shooting points near local buildings. Three sweeps were selected for default number of sweeps, however, we set a specific shooting point where a larger number of sweeps from eight to twelve were applied for the purpose of high seismic energy transmission to enhance seismic illumination and high signal to noise ratio of both reflection and refraction events.

Installed survey lines are shown in Figure 6, most of which were deployed along local agricultural roads. Stand-alone measurement equipments in some residential zones are indicated by red dots.

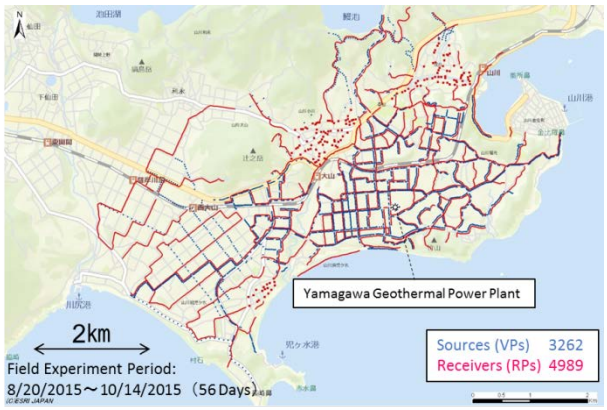

Figure 6: Survey line deployment of Yamagawa seismic survey project.

2.4 Seismic Data Processing

Acquired seismic data was processed by reference to the flow shown in Figure 7. Reflection data processing were conducted in parallel with refraction data analysis. We referred the output of refraction tomography for stacking velocity analysis.

Since there is no single algorithm that can reduce all types of noise in seismic data, several types of noise reduction methods were applied. Figure 8 shows the flow of noise reduction steps. We conducted careful parameter testing and tried some patterns of order of noise reduction process. F-X (frequency-space) edit reduces the noise with specific frequency by detecting the anomalous data in frequency-space (F-X) domain within analysis window, and replacing the data with predicted signal of the window (Guo and Lin, 2003). Data adaptive time variant filter (DATVF) reduces an eccentrically-located noise by scaling anomalous amplitude to the same level of the other data within the analysis window in the frequency domain (Elboth et al., 2008). F-X prediction filter removes random noise and enhances continuity of reflected wave signal. This process replaces noise component with signal that is predicted based on amplitude distribution in F-X domain. F-X prediction filter has an efficacy by applying on both domains of common shot and receiver gathers (Gulunay,1986). F-X velocity filter suppresses linear noise in the shot gather such as surface wave and refracted wave. F-X velocity filter models a linear noise by extracting steep linear noise signals of the shot gather by the method of least squares in the F-X domain.

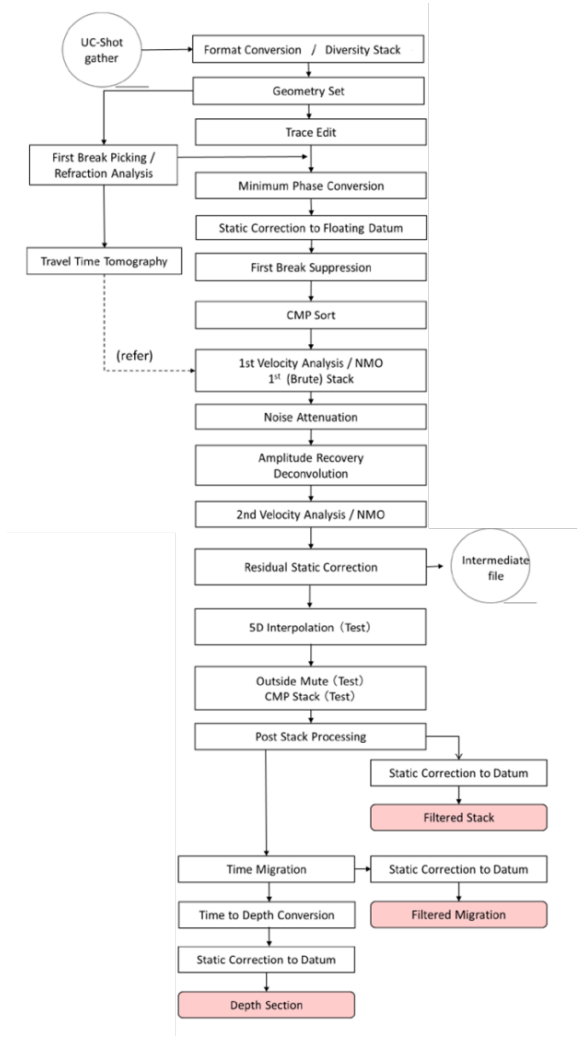

Figure 7: Processing flow for 3D seismic data.

We tried out 5D interpolation technique to apply to the 3D seismic volume to interpolate the data gap and to achieve an even trace distribution interval. Even trace distribution has several effects on seismic data quality such as a reduction of migration noise and acquisition footprints. 5D interpretation is the processing method that corrects an effect of irregular acquisition geometry and predicts a missing data in the survey area. In our processing, 5D interpolation method with the minimum weighted norm interpolation (Liu and Sacchi, 2004) was applied. In the processing, weighting function is calculated based on five dimensional power spectrum estimated from four spatial dimensions (Inline, Cross-line, Offset, Azimuth), and temporal dimension (Time or Frequency). Then, missing data is interpolated by the minimum norm method.

Figure 9 shows the effect of 5D interpolation. A data gap at shallow zone is filled with reasonable interpolated signals, and random noises were eliminated at deeper part.

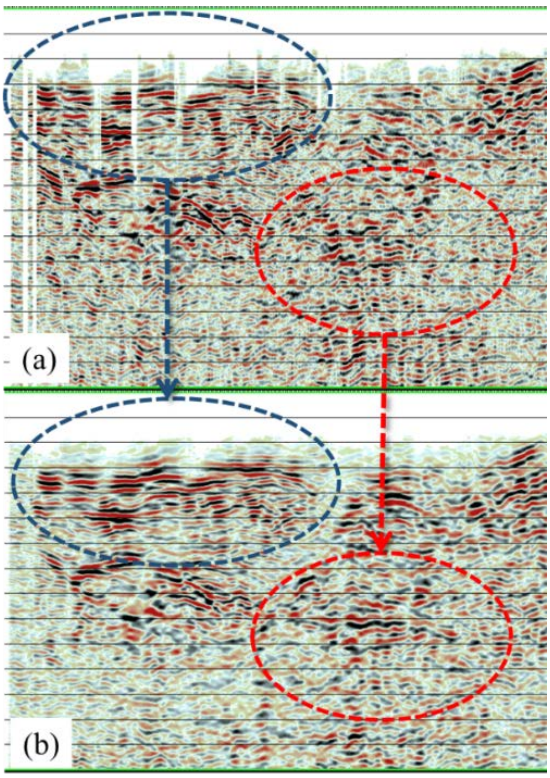

Figure 9: (a) Original cross section and (b) the result of 5D interpolation.

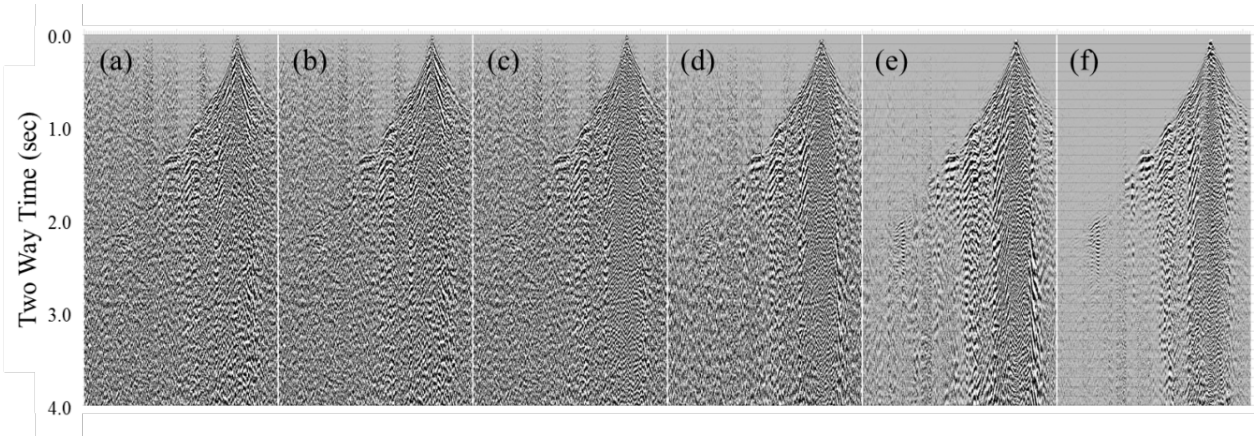

Figure 8: Shot gather comparison among the noise reduction steps. (a) Original shot gather. (b) F-X edit processed data. (c) DATVF, (d) F-X prediction filter, (e) F-X prediction filter applied on receiver gather, (f) F-X velocity filter. All processing was applied on shot gather except for (e). Maximum straight-line distance of each shot gather is approximately 8 km.

Seismic survey lines with irregular geometry are expected at mountainous area where the number of road is limited. The geometry causes the data gap and irregular interval of seismic traces. Therefore, we consider the 5D interpolation is one of the key processing to improve quality of seismic data acquired with irregular survey geometry.

We applied post-stack time migration for seismic imaging that is confirmed in the reprocessing verification test in 2013. Smoothed stacking velocity is used to depth conversion for final seismic depth volume.

2.5 Seismic Interpretation

We interpreted depth converted post-stack time migration data. Figure 10 shows 2D seismic cross section. We can detect the depression structure of the Nansatsu formation in seismic section which is assumed in the geological conceptual model, although there is a misalignment of deepest portion of depression. Assumed faults and the dacite body are not clearly visible in this section but the spread of positive high amplitude seismic event possibly indicates the top of dacite, the depth of which was confirmed by well information.

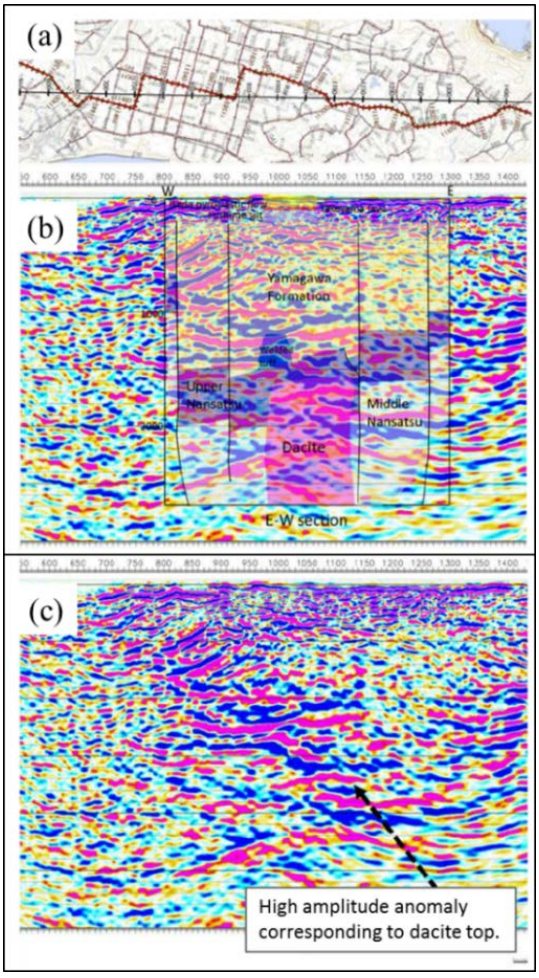

Figure 10: Comparison of the 2D seismic cross section and the existing geological schematic cross section (after Sakuma, 1999). (a) 2D seismic line location map, (b) 2D seismic section with superimposed schematic cross section of Figure 3. (c) Same seismic cross section without the transparentized geological interpretation.

We conducted 3D seismic interpretation by reference to comprehensive structure estimated on the 2D seismic section. Six wells were referred for the geological interpretation and careful well confrontation was conducted on the arbitrary crooked cross section (Figure 11).

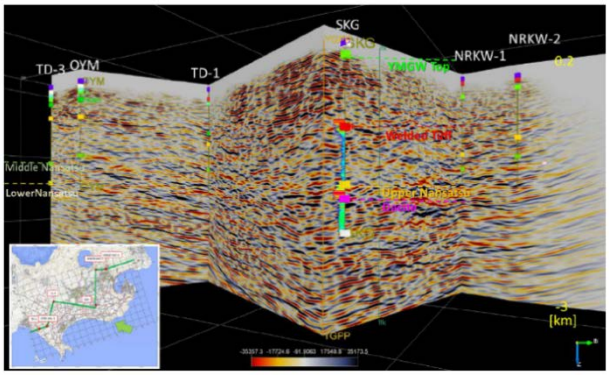

Figure 11: Arbitrary crooked cross section extracted from 3D seismic volume. The arbitrary line connects the existing well locations. Observing point is southeastern side of the survey area.

In the interpretation, we also utilized the difference in vision that is due to a difference in the frequency range for verification of assumed geological horizon. Figure 12 shows an example of the verification. Depression structure indicated by large amplitude is highlighted by low pass filter with 8 Hz corner frequency and it would help address to interpret the depression structure in large scale, although detailed structure has been filtered out.

Figure 13 shows the 3D view of interpreted surface structure for the top of the upper Nansatsu formation. The depression structure that is consistent with the previously thought by existing surveys except the larger depression structure exists along Tujinodake-Takeyama structural line.

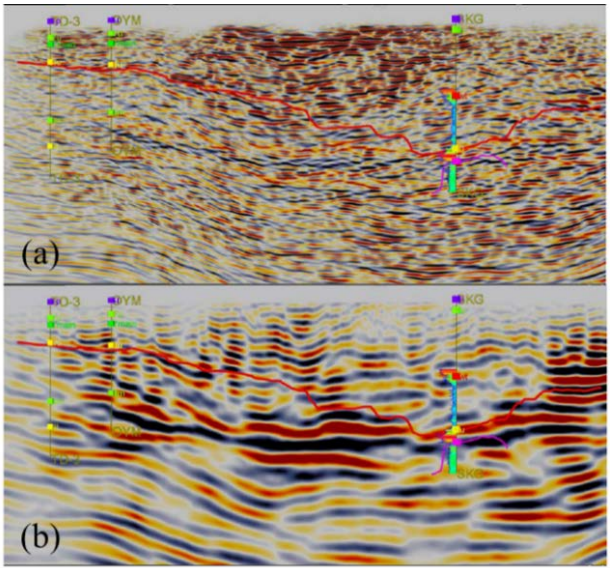

Figure 12: Comparison of seismic cross sections. (a) Original seismic cross section, (b) Band limited cross section with 8Hz low pass filter. Red line shows the interpreted top horizon of Upper Nansatsu formation.

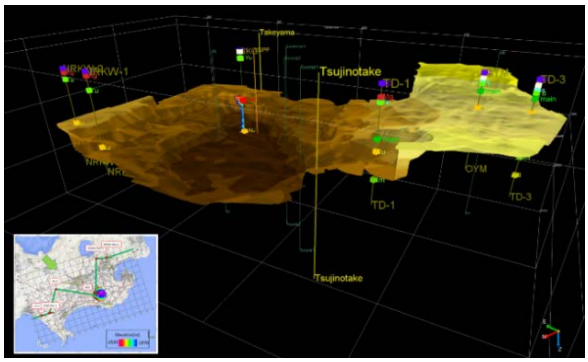

Figure 13: 3D view of interpreted seismic horizon of the upper Nansatsu formation. The yellow vertical lines represent the locations of Takeyama and Tsujinodake peakes.

2.6 Velocity Tomography

3D refraction tomography was also applied to 3D seismic data to evaluate shallow velocity structure of Yamagawa geothermal field. Figure 14 shows the top view of the 3D volume-sculpted image of the interval velocity model. In this figure, interval velocity less than 3,100 m/s is transparentized at elevation ranging from 200 to -500m. Tongue-shaped high velocity anomaly expanding toward south-southeast is clearly observed. 3D view of volume-sculpted image is shown in Figure 15. Several high velocity layers lay on top of each other. During data acquisition, southern part of high velocity anomaly zone was considered as seismic energy attenuation zone since the seismic signals are poorly observed beyond the area on the shot gather. It is supposed to be that the shallow high velocity anomaly distorted the seismic ray paths.

There are some signatures of volcanic activities such as Ikeda caldera lake and Unagi-ike maar in the direction of possible roots of the high velocity anomaly volume. These aspects indicate that the anomaly reflects a possible lava flow of circumjacent volcanic activities. According to well information, the shallowest high velocity anomaly sheet is contrasted with Gongen-yama pyroclastic rocks of Ata volcanically active period in the late Pleistocene (NEDO, 2001). Further investigation is desired to verify the assumption for the deeper understanding of the relationship between the velocity structure and the volcanic activities.

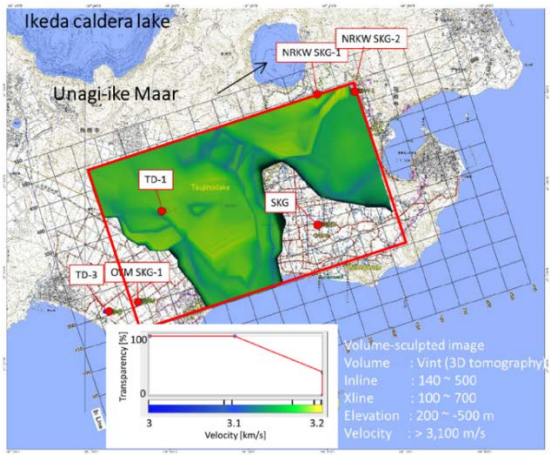

Figure 14: Map view of 3D refraction velocity tomography results. Velocity volume less than 3,100 m/s is transparentized within the red rectangle.

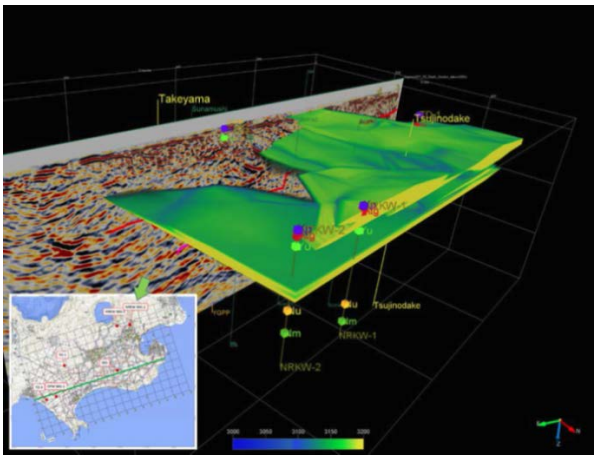

Figure 15: 3D view of volume-sculpted image of Figure 14. Observing point is northeastern side of the survey area. Color scale and transparency setting is same as Figure 14. Elevation range for 3D display is from 200 to -500m.

2.7 Coherency Analysis

We conducted coherency analysis on the post stack time migration data volume, and extracted the distribution of discontinuity of reflection seismic waves. Coherency attribute is used as an index for discontinuity structure, and spotlighted recently in fracture estimation of shale gas reservoirs. Semblance is one of the evaluation indicator of coherency analysis. Semblance value at good seismic continuity location values close to 1. Figure 16 shows the semblance distribution on the surface slice of the top upper Nansatsu formation.

Figure 17 shows the semblance anomaly with a spatial reference of dacite intrusion and injection zone. Semblance anomaly distributes around the estimated dacite structure and in the injection zone. In addition, we can see the alignment of semblance along the Takeyama-Tsujinodake structural line but only vaguely.

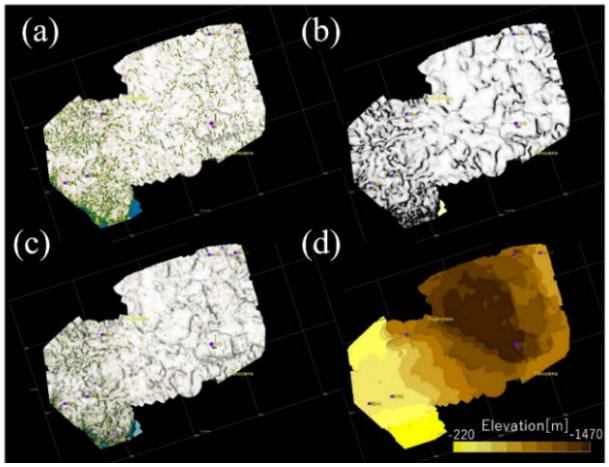

Figure 16: Semblance distributions on the surface slice of upper Nansatsu formation top. (a) Semblance distribution analyzed on original seismic volume. Color scale of (a) is adjusted to show green color when the semblance value below 0.8. (b) 8 Hz low pass filtered volume. Color scale is adjusted to show black color when the semblance value below 0.3. (c) Co-rendered semblance distribution of (a) and (b). (d) Elevation map of top upper Nansatsu formation.

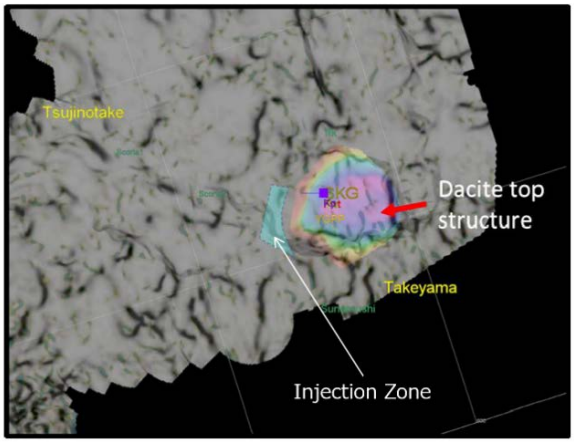

Figure 17: Comparison of semblance anomaly (Figure 16 (c)) and interpreted top structure of dacite intrusion.

3. DISCUSSION

The consistency of semblance distribution and existing information confirmed by well drilling and/or geological surveys is encouraging result, however, further numerical evaluation should be conducted to discriminate a large number of candidates distributed around the geothermal power station and select the possible permeable fracture indication for drilling target determination.

Refraction velocity tomography analysis unveiled the shallow high velocity anomalies indicates possible evidence of volcanic activities such as lava flow. In the past, large faulting which drops nearly 1,000 meters is interpreted based on gravity survey analysis at the western part of depression structure of the Nansatsu group. On the other hand, it is not clear that the large fault boundary of top of the upper-Nansatsu formation in our seismic interpretation. Eastern edge of the tongue-shaped distribution of the shallow high velocity anomaly coinsides with the interpreted fault line based on gravity anomaly. If the high velocity anomaly is caused by geological formation with high density rocks, the gravity data could have been affected by this shallow high velocity anomaly (Figure 18). This discovery will raise a question about the current geothermal exploration style depending on geophysical surveys other than seismic methods. It will be required to apply a composite exploration method including several geophysical survey for geologically complex survey field.

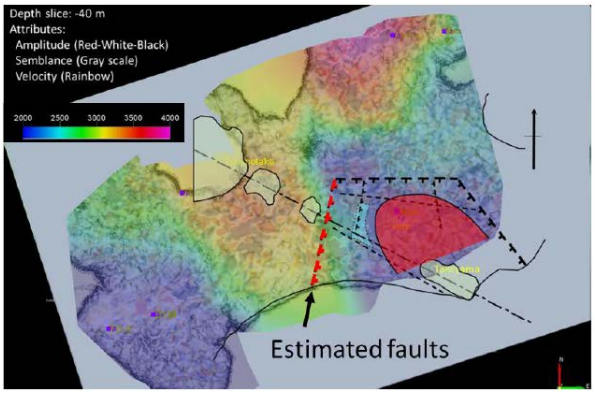

Figure 18: Comparison of high velocity anomaly distribution and estimated fault location (Sakuma, 1999) based on gravity data.

4. CONCLUSION

An efficacy of the application of seismic method to geothermal reservoir exploration has been questioned for a long time. However, our 3D seismic survey project showed the possibility to unveil the detailed geothermal reservoir structure by the latest seismic technologies. In the next phase from 2016 to 2017, we will apply a quantitative evaluation and spatial distribution analysis on the coherency attributes. Detailed accuracy evaluation of coherency analysis will give us indications to distinguish the possible reservoir zone and phantom structure. Then spatial distribution of permeable fracture reservoir indicators will help to address to construct the realistic geothermal reservoir model for efficient fluid flow simulation.

In addition, we are going to take the integration geophysical survey concept into account, which improves accuracy with referring the different geophysical property estimated by the other methods each other. Comprehensive data analysis is planned in the next phase with using gravity and MT(Magneto-Telluric) data which is acquired at the Yamagawa geothermal field.

Encouraging results of Yamagawa 3D seismic survey is further than the achievement that gained at the suitable field for 3D seismic survey. We would like showing similar results in the mountainous region where the most of the geothermal resources are unevenly distributed in. Therefore, we plan the second experimental seismic survey in a mountainous region with applying these achievements in the next two years. Results and knowledges of this program will be summarized in a guidebook as a tutorial for geothermal developers who consider the application of seismic method for geothermal reservoir imaging. We would be most happy if our accomplishments will lead to future development of geothermal exploration and reservoir evaluation.

ACKNOWLEDGEMENTS

The authors would like to thank great cooperation of various related parties of local government and local residents. The authors also thank Kyushu Electric Power Co., Inc., West JEC and JAPEX for the provision of prior survey results and geological information around the power station.

REFERENCES

Elboth T., Fugro Geoteam, Qaisrani H.H. and Hertweck T.: De - noising seismic data in the time - frequency domain. SEG Technical Program Expanded Abstracts 2008, 2622-2626, (2008).

Geospace Technologies: Geospace Seismic Recorder (GSX), [online] 1st Oct. 2012 Available at http://www.geospace.com/geo- space-seismic-recorder-gsx/, [Accessed 5 August 2016].

Gulunay N.: FXDECON and complex wiener prediction filter. SEG Technical Program Expanded Abstracts 1986, 279-281, (1986).

Guo J. and Lin D.: High - amplitude noise attenuation. SEG Technical Program Expanded Abstracts 2003, 1893-1896, (2003).

Horikoshi, T., Uchida, T., Oketani Y., Hisatani K. and Nagahama N.: NEDO's Development of Fracture-Type

Reservoir Exploration Technology, Proc. 18th NZ Geothermal Workshop, (1996).

Liu, B. and Sacchi, M.D.: Minimum weighted norm interpolation of seismic records, Geophysics, 69, 6, 1560-1568, (2004).

Matumoto, T.: The four gigantic caldera volcanoes of Kyusyu, Japanese journal of geology and geography, vol. 19, Special number, p1-57, (1943).

New Energy and Industrial Technology Development Organization (NEDO): Geoscientific Study in the Tsujinodake Area, Kagoshima Prefecture, on the Geothermal Development Promotion Survey Project (in Japanese with English Abst.), (2001)

Okada, H., Yasuda Y., Yagi M., and Kai K.: Geology and fluid chemistry of the Fushime geothermal field, Kyusyu, Japan, Geothermics, 29, 279-311, (2000).

Sakuma, K.: Development and Present Status of the Yamagawa Geothermal Field, Jour. Geotherm. Res. Soc. of Japan, 21, 3, 291-297, (in Japanese with English Abst.) , (1999).

Thermal and Nuclear Power Engineering Society: Current Status and Trend Geothermal Power Generation 2015 (in Japanese), (2016)

Tosha, T., Shimada, T. and Nakashima H.: The Research and Development for the Geothermal Energy in JOGMEC, Proc. World Geotherm. Cong. 2015, Melbourne, Australia, 19-25 April 2015, (2015).

Yoshimura, Y., Yanagimoto Y. and Nakagome, O.: Assessment of the geothermal potential of the Fushime area, Kyushu, Japan. Journal of the Japan Geothermal Energy Association 22, 167-194, (in Japanese with English Abst.), (1985).